Design and Operation of a Thrust Test Stand for University Small Satellite Thrusters

Terry Stevenson[1] and Glenn Lightsey[2]

Georgia Institute of Technology, Atlanta, GA, 30332

A small, low cost thrust test stand was developed at the Georgia Institute of Technology to support ongoing small spacecraft propulsion research. The test stand is a torsional pendulum with a low natural frequency, designed to respond to thruster pulses in the range of milliseconds to hundreds of milliseconds as if they were instantaneous impulses. The stand displacement is measured by an LVDT, and the magnitude of the oscillation resulting from the thrust is used to determine the impulse delivered. The stand is not actively damped, and is operated with less time between impulses than the oscillations take to decay. A post-processing method was developed to separate the oscillation caused by an impulse from the previous oscillations, by fitting a damped oscillator equation before and after the impulse, and determining the instantaneous angular velocity change across the impulse. The stand was used to test a thruster developed at Georgia Tech for the NASA BioSentinel mission.

I. Nomenclature

b	LVDT bias
c	Stand arm damping coefficient
g	Standard acceleration due to gravity (9.806 m/s^2)
I	Mass moment of inertia of the stand
Isp	Specific impulse
J	Impulse
k	Flex pivot torsional spring rate
k_{eff}	Effective torsional spring rate, including gravitation term
L_L	Distance from LVDT to axis of rotation
L_T	Normal distance from thrust vector to axis of rotation
LVDT	Linear Variable Differential Transducer
m	Mass of the test stand arm
Δm	Change in mass of the thruster due to propellant consumption
s	Sensitivity of the LVDT
Δt	Duration of a thruster actuation
T_{avg}	Average thrust over a short impulse
t_f	Time at which the thruster begins firing
V	LVDT voltage
x_{COM}	Location of the test stand center of mass relative to the axis of rotation
ζ	Damping ratio of the stand
θ	Angular deflection of the stand in the horizontal plane
ϕ	Angular offset of the stand from the horizontal plane
ω_n	Natural frequency of the stand

---

[1] Graduate Student, Georgia Institute of Technology, AIAA Student Member
[2] Professor, Georgia Institute of Technology, AIAA Fellow

II.   Introduction

Thrust test stands are critical tools in the development of spacecraft propulsion systems, as they allow experimental verification of the thrust and specific impulse of a propulsion system before flight. The need for such facilities is growing, as more universities [1] and small companies [2] are creating custom propulsion systems for CubeSats and other small satellites. A small, low-cost thrust stand was designed and built to support CubeSat propulsion research at the Georgia Institute of Technology's Space Systems Design Lab (SSDL). The test stand was then used to measure the performance of a cold gas attitude control thruster for NASA's BioSentinel mission.

III.   Test Stand

A. Vacuum Chamber

The stand is installed in the SSDL's small vacuum chamber, made by LACO Technologies. The chamber is a stainless steel cube with a 61 x 61 x 61 cm interior. The chamber uses a Laybold Turbovac 350ix turbomolecular pump to achieve a base pressure of 10^{-6} Torr, and a LACO W2V40 rotary vane pump both for roughing the chamber and for backing the turbopump. Chamber pressure is measured by an INFICON Gemini MPG500 Pirani/Cold Cathode pressure gauge. While the chamber does not have a large internal volume, it can be pumped to vacuum quickly: a typical cycle requires 20 minutes to reach 10^{-5} Torr. The chamber is shown below in Figure 1.

Figure 1: SSDL vacuum chamber

B. Test Stand Design

The thrust stand is a torsional pendulum design [3]. The stand consists of a stationary frame that supports a rotating arm, which supports the thruster. Impulse from the thruster causes the arm to rotate, and a restoring force produces an oscillation in the arm. The impulse delivered is calculated from the amplitude of the oscillation. The stand is based on a test stand designed and built at NASA Glenn Research Center for testing pulsed plasma thrusters

American Institute of Aeronautics and Astronautics

[4]. The Glenn test stand is much larger than the vacuum chamber available to the SSDL, and too expensive to reproduce. The SSDL test stand is smaller, and is fully automated, to allow long test sequences to run without direct supervision.

This test stand was designed to measure low thrust levels for short periods of time; the reference minimum impulse design was a 40 mN thrust lasting for 3 milliseconds, for an impulse of 120 μN-s. Measuring the entire time-varying thrust profile over such a short duration is extremely difficult with a pendulum-style test stand. The stand would require a sub-millisecond response time, which requires a stand that is either very stiff or lightweight. The dynamic portion of the thrust stand must include the thruster itself, which limits how lightweight it can be. The high required stiffness would reduce the magnitude of the stand's motion, which in turn reduces the resolution of the stand. Instead, this test stand was designed to have a much longer response time than the duration of the thrust, approximately 10 seconds. Such a stand responds to a 3 millisecond thrust duration as if it were an instantaneous impulse. This allows a low stiffness, and relatively large oscillation amplitude, which improves the resolution of the stand.

The stand is shown installed in the SSDL vacuum chamber in Figure 2, with some key pieces of the stand highlighted. The blue vertical axis can rotate relative to the frame, and is attached to the orange bar, which can rotate in the horizontal plane. The purple bracket on the right side of the image connects the thruster to the horizontal arm. The bracket can be easily replaced to adapt the stand to test other thrusters with different geometries or mounting points. The stand counterweights are highlighted in green, and the Linear Variable Differential Transformer (LVDT) mounting block is shown in cyan. A simplified schematic of the rotating segment of the stand is shown in Figure 3.
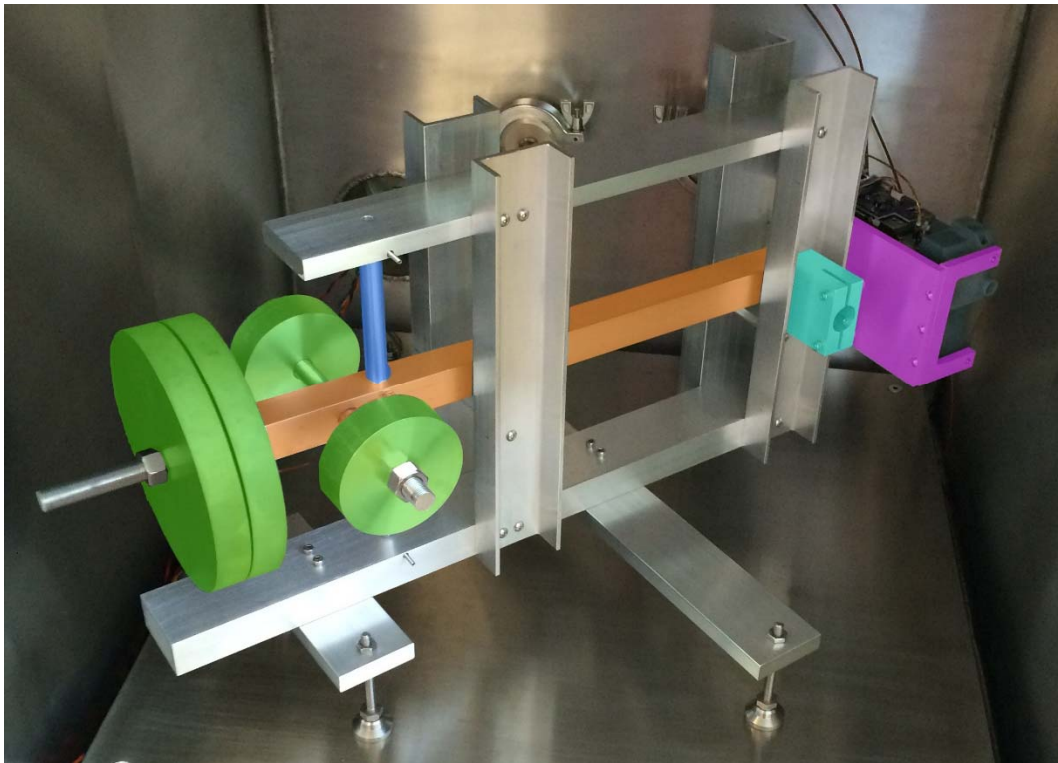
Figure 2: Test stand installed in the SSDL vacuum chamber, key elements highlighted for visibility
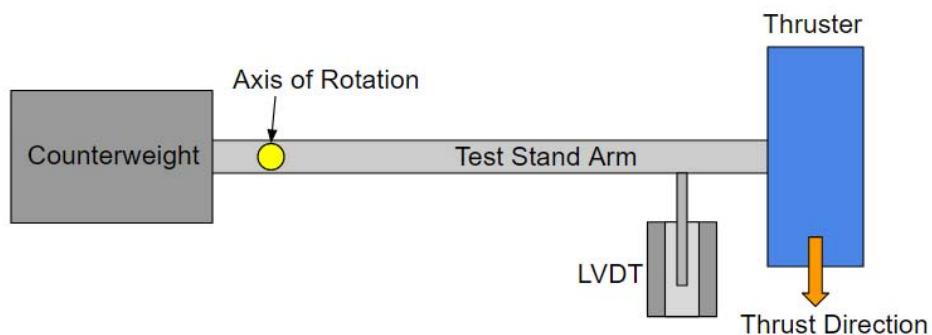
Figure 3: Schematic of the test stand's rotating components.

The rotating axle is connected to the frame of the stand with two flex pivots. Each flex pivot consists of two concentric cylindrical sleeves, connected by perpendicular leaf springs. The sleeves can rotate about their common axis up to 30 degrees, and there is no contact between the sleeves other than the leaf springs. The flex pivots have several advantages over conventional bearings in this application. They require no lubrication, which simplifies operation in vacuum; they are nearly frictionless, with negligible static friction; and the leaf springs provide a built-in restoring torque, eliminating the need for a separate torsion spring. A CAD image of a flex pivot is shown in

American Institute of Aeronautics and Astronautics

Figure 4, note that the outer sleeve is separated into two cylinders. One end of the pivot is fixed in the stationary frame, and the other end is fixed in the axle.

Figure 4: CAD image of a flex pivot

The three counterweight wheels are used to balance the thruster and keep the center of mass of the rotating segment near the axle. The hub of each wheel is threaded, allowing them to be precisely positioned. In practice, the arm is deliberately not completely balanced, and the center of mass is located approximately 2-4 cm away from the axle in the direction of the thruster. This allows the leveling feet to be used to set the zero point of the stand. This introduces additional restoring torque, which is lumped together with the restoring torque of the flex pivots.

An LVDT is used to measure the deflection of the stand. In this case, a Macro Sensors DC-750-125 with a range of ± 3.175 mm is used. An LVDT requires no contact between the core and the housing, so no additional friction is introduced in the system. The axial position of the magnetic core within the housing determines the output coil voltage of the housing, which is measured at 1000 Hz by a National Instruments USB-6002 DAQ. The LVDT is held in place in the stationary frame by a bracket, and the core is held on a threaded rod attached to the rotating arm.

C. Dynamics

The angular deflection θ of the arm is computed from the LVDT voltage with:

$$\sin \theta = \frac{V}{s L_L} \tag{1}$$

where V is the LVDT output voltage, s is the sensitivity of the LVDT (in volts/millimeter), and L_L is the perpendicular distance from the axis of rotation to the LVDT core. The maximum angular travel of the stand is only 1.2° from the neutral position, so the small angle approximation is used:

$$\theta = \frac{V}{s L_L} \tag{2}$$

When the thruster is fired, the impulse on the stand causes it to rotate, starting an oscillation in the arm with a period of approximately 10 seconds. Since this period is three to four orders of magnitude longer than the typical thrust duration, the stand responds as if it were an instantaneous impulse. The arm of the stand behaves as a damped oscillator, described by:

$$I\ddot{\theta} + c\dot{\theta} + 2k\theta + mg x_{COM}\phi\theta = 0 \tag{3}$$

where I is the mass moment of inertia of the entire rotating segment of the stand, including the thruster and counterweights; $\ddot{\theta}$ is the angular acceleration; $\dot{\theta}$ is the angular velocity; θ is the stand deflection; c is the damping coefficient of the stand; k is the spring constant of one of the flex pivots (doubled because there are two flex pivots on the axle); m is the mass of the rotating segment; g is the acceleration due to gravity; x_{COM} is the location of the rotating segment's center of mass relative to the axle; and ϕ is the angle that the stand arm makes with the horizontal plane when in the neutral position. The final term accounts for the extra restoring torque the arm experiences due to the center of mass offset. In order to set the zero position with this method, the arm is not perfectly level in the horizontal plane. The angles ϕ and θ are small, and the small angle approximation is used here. These two angles are illustrated in Figure 5, below.
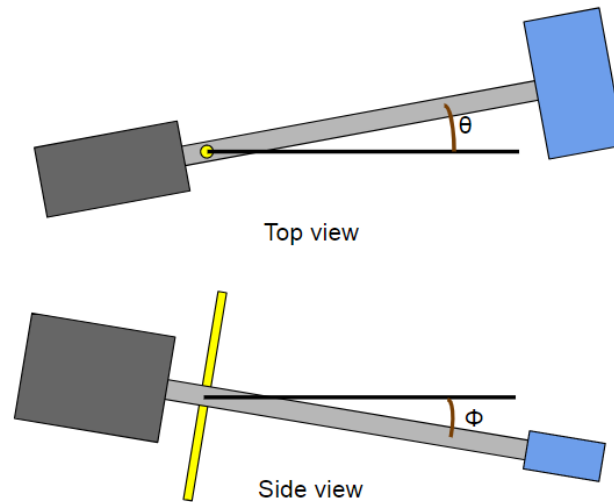
Figure 5: θ and ϕ, illustrated on the test stand. Angles are exaggerated for clarity

The two restoring torque terms can be collected into an effective spring rate:

$$I\ddot{\theta} + c\dot{\theta} + k_{eff}\theta = 0 \qquad (4)$$

$$k_{eff} = 2k + mgx_{COM}\phi \qquad (5)$$

The angle ϕ and the center of mass location are difficult to measure in practice, so the effective spring rate term is estimated from the data as a single term. Following the conventional solution to the pendulum problem, the equation is divided by the moment of inertia, and the resulting terms are consolidated into damping ratio and natural frequency:

$$\ddot{\theta} + \frac{c}{I}\dot{\theta} + \frac{k_{eff}}{I}\theta = 0 \qquad (6)$$

$$\ddot{\theta} + 2\zeta\omega_n\dot{\theta} + \omega_n^2\theta = 0 \qquad (7)$$

where ζ is the system damping ratio, and ω_n is the natural frequency. The characteristic solution to Eq. (7) is:

$$\theta(t) = Ae^{-\zeta t}\cos(\omega t + \phi) + b \qquad (8)$$

American Institute of Aeronautics and Astronautics

where A is the amplitude at t=0, ϕ is the phase of the oscillation at t=0, and b is the mean, or bias, of the oscillation. Note that Eq. (8) is only valid in the absence of external forces, as evidenced by the right hand side of Eq. (7) being zero. Therefore, the equation is only valid when the stand is oscillating freely and the attached thruster is not firing.

In order to simplify the stand, no active damping is used. Due to the low passive damping of the system and the high sensitivity of the LVDT, the oscillations from a typical firing are detectable for up to fifteen minutes before decaying into the background noise. To achieve a higher pulse rate during testing, the thruster is fired approximately every 60 seconds, adjusted up or down depending on the mass of the thruster being tested. Therefore, at each pulse time, the stand is still oscillating from the previous pulse. The two oscillations are separated when processing the data, as detailed in the next section. The pulse rate is chosen to avoid resonance with the period of the stand, which is dependent on the mass of the thruster being tested. For example, when testing the 1.2 kg BioSentinel thruster, the stand period was 10.2 seconds, and the pulse spacing was chosen to be 65 seconds.

The test stand operates autonomously once the thruster is installed and powered, which allows long test sequences consisting of thousands of individual firings to be run without operator supervision. A MATLAB script is used to read LVDT voltage measurements from the DAQ, send commands to the thruster over a serial port, and collect thruster telemetry. A typical test will involve operating the thruster at a range of different pulse widths, which are provided to the MATLAB script in a configuration file. Thruster telemetry is acquired before each pulse, and is saved along with the raw data. This includes propellant tank pressure and temperature, along with thruster health data.

IV.   Data Processing

As discussed above, the applied thrust duration is significantly shorter than the period of the test stand, so the thrust is effectively an instantaneous impulse. This impulse is treated as a discontinuity in the angular velocity of the stand. The stand behaves like a free oscillator before and after this impulse, and its motion can be described by the equations derived above. LVDT measurements are collected and converted to angular measurements for 30 seconds before and after each pulse. The equation of motion of the stand, Eq (8), is applied piecewise to the angle measurements, separated at the time of the thruster's pulse:

$$\theta = \begin{cases} \theta = A_1 e^{-\zeta t} \cos(\omega t + \phi_1) + b & t < t_f \\ \theta = A_2 e^{-\zeta(t-t_f)} \cos(\omega t + \phi_2) + b & t \geq t_f \end{cases} \quad (9)$$

These equations are fit to each displacement series using a least squares method, and are constrained to be equal at $t = t_f$, since only the velocity, not the angle, is discontinuous. The instantaneous change in angular velocity is treated here as a change in amplitude and phase, with the other parameters remaining constant.

In order to fit Eqs. (9) to the data, eight parameters must be estimated: A_1, A_2, ζ, ω, t_f, ϕ_1, ϕ_2, and b. Of these, four are relatively simple to estimate. ζ and ω are properties of the stand, and do not change greatly from test to test, thus their initial "guess" values are quite close to the true values. There are gradual changes in these values during the course of a test, due to the changing mass of the system from propellant consumption, so they are still estimated for each firing. Likewise, the bias b can be given a close initial guess by taking an average of all peak and trough

angles. The time of firing t_f is controlled by the MATLAB script, although it is still estimated, to allow for a case in which there is a latency between the thruster command and the start of the pulse.

In order to determine the impulse, the angular rate of the stand before and after the pulse is needed. This is determined by differentiating Eq. (8), the stand's equation of motion:

$$\omega = \frac{d\theta}{dt} = -A\zeta e^{-\zeta t}\cos(\omega t + \phi) - A\omega e^{-\zeta t}\sin(\omega t + \phi) \qquad \textbf{(10)}$$

The estimated parameters are applied to Eq. (10) at $t = t_f$ to determine the angular velocity immediately before and after the impulse. The difference in these angular velocities is used to determine the impulse applied to the stand, using:

$$J = \frac{I\Delta\omega}{L_T} \qquad \textbf{(11)}$$

where J is the delivered impulse, I is the moment of inertia of the rotor, $\Delta\omega$ is the angular velocity change, and L_T is the perpendicular distance from the axis of rotation to the thruster nozzle.

The uncertainty in the impulse measurement can be found using:

$$\sigma_J^2 = \sigma_I^2 \left(\frac{\Delta\omega}{L_t}\right)^2 + \sigma_{\Delta\omega}^2 \left(\frac{I}{L_t}\right)^2 + \sigma_{Lt}^2 \left(\frac{I\Delta\omega}{L_t^2}\right)^2 \qquad \textbf{(12)}$$

where σ_J, σ_I, $\sigma_{\Delta\omega}$, and σ_{Lt} are the uncertainties in impulse, moment of inertia, angular velocity change, and nozzle distance, respectively. The uncertainty in the location of the thruster nozzle relative to the stand axle is primarily due to the integration of the thruster on the stand bracket. In the case of the BioSentinel thruster, the maximum error in the thruster nozzle position relative to the axle was ± 0.4 mm. The thruster was mounted on the bracket with four fasteners that had some freedom to move within their clearance holes, this contributed the majority of the error (0.35 mm). The remainder was uncertainty in the true length of the stand arm and the bracket.

The uncertainty in the mass moment of inertia is more significant. The stand arm itself is well characterized, and the position of each counterweight is measured before a test. The mass of the thruster is measured before and after each test, and the propellant consumption is assumed to be distributed evenly between pulses. For example, a 1000 pulse test that resulted in a total mass loss of 2 grams would be processed as if the mass of the thruster decreased by 2 milligrams per pulse. In the case of tests involving pulses of different durations, the mass consumption is assumed to be proportional to duration. The metal parts of the stand were individually massed to confirm CAD predictions, which were then used to determine the moments of inertia. This carries the assumption that the materials used have uniform densities and are manufactured according to spec. The parts were thoroughly inspected after machining, and were either aluminum or stainless steel, so the assumption of uniform density is a reasonable one. The largest contributor to the uncertainty is the propellant distribution within the thruster's tanks, in part due to the thruster's location at the end of the arm, far from the axis of rotation. The unusual shape of the propellant tank in the BioSentinel thruster was especially significant. Overall, the mass moment of inertia uncertainty was between 2% and 6%, depending on how much propellant was loaded into the system.

Finally, the uncertainty in the angular velocity change is determined by using the covariance matrix produced by the least squares estimation process. The uncertainties in the estimated terms are applied in a standard error propagation equation derived from the stand's angular velocity equation. This equation is not reproduced here due to

American Institute of Aeronautics and Astronautics

excessive length. Due to the long measurement time of the system and the large number of voltage readings collected, this error is small, typical values are between 0.1% and 1% of the total change.

Of these three uncertainties, the most significant by far is the mass moment of inertia. The term associated with that error, the first term of the right hand side of Eq. (12), is typically an order of magnitude higher than the angular velocity uncertainty term, and two to three orders of magnitude higher than the nozzle distance uncertainty term. A typical test using the BioSentinel thruster produced an impulse estimate of 1.08 ± 0.04 mN-s. Smaller impulses typically have larger uncertainty relative to the impulse magnitude: a shorter pulse width produced an estimate of 0.21 ± 0.012 mN-s.

Dynamic calibration of the test stand to more precisely determine the moment of inertia of the system is planned for future iterations of the design. A lightweight swinging hammer will be fixed to the test stand, pulled back by a motor and allowed to swing freely and impact the stand arm. Proper characterization of the mass and moment of inertia of the hammer will allow more precise impulse estimates to be made.

V.   Thrust Measurements

The test stand was used to test a cold gas attitude control thruster developed for the BioSentinel mission [5]. This thruster produces pulse durations between 3 and 200 milliseconds, with an average thrust of 40 mN. The thruster was fired on the test stand more than 40,000 times over the course of two test campaigns. It was operated with a wide range of pulse durations, ambient temperatures, and propellant pressures. A typical LVDT voltage plot during one of the BioSentinel thruster's 50 millisecond pulses is shown in Figure 6. Note the oscillations from the previous firing, and the near-instantaneous change in angular velocity. No smoothing has been applied to the voltage seen in Figure 6.
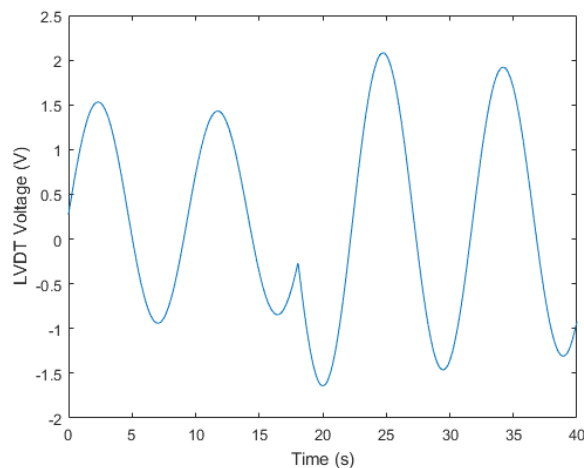
Figure 6: Test stand LVDT voltage during a 50 ms, 40 mN thruster pulse.

This test stand only measures the total impulse of a given firing, however, values for average thrust and specific impulse can also be determined. This average thrust is computed with:

$$T_{avg} = \frac{J}{\Delta t} \quad\quad\quad\quad (\,13\,)$$

American Institute of Aeronautics and Astronautics

where T_{avg} is the average thrust, J is the impulse, and $\varDelta t$ is the duration of the pulse. The $\varDelta t$ here is the commanded duration of the pulse. Using the commanded duration brings with it two critical assumptions. The first major assumption is that the valve driving electronics function perfectly, and apply power to the valve for exactly the commanded duration. In general, this is not a bad assumption. For example, the BioSentinel thruster was found to have an upper bound timing error of 10 microseconds.

The second assumption is that the thrust is constant while valve power is applied, and zero otherwise. An actual system would be expected to have a roughly trapezoidal thrust profile, with an initial rising period as the valve opens, and a final falling period as it closes. Since the exact shape of this profile is unknown and cannot be determined with this test stand, it is simply assumed to be rectangular, with instant opening and closing of the valves. This assumption is good when the commanded duration is large compared to the opening and closing times of the valves, or when the opening and closing times are nearly identical. However, if the valve takes substantially longer to close than to open, the system will experience an apparent increase in average thrust at shorter pulse times. This is illustrated in Figure 7. The bold lines show the true thrust profile for the two pulses. The red region represents the lost impulse due to the finite opening time of the valves, while the green region represents extra impulse due to the finite closing time. Since the closing of the valve is slower than its opening, each pulse gains some impulse, which has a proportionally larger effect on the short pulse.
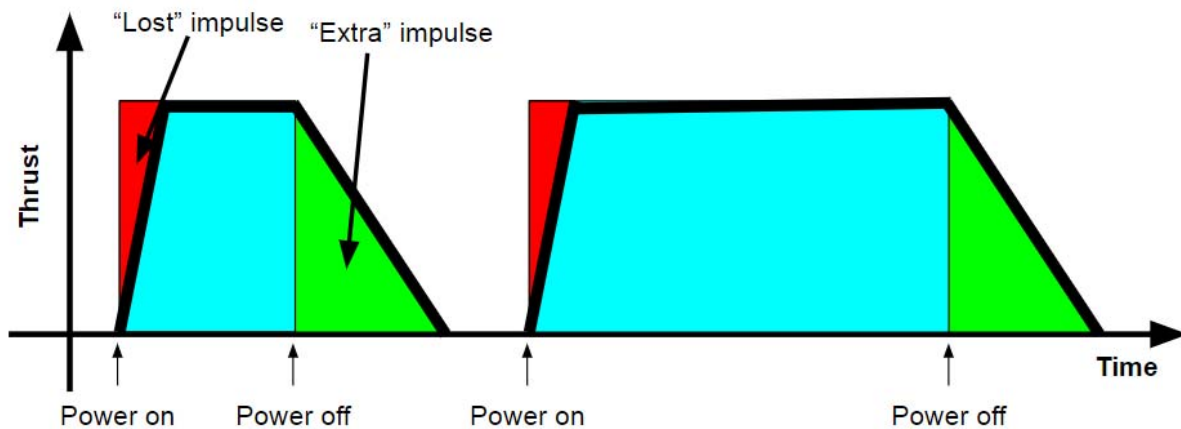
Figure 7: Notional plot of thrust profile for a short and long pulse, the bold line represents the true thrust.

Calculation of specific impulse (I_{sp}) is more straightforward. The specific impulse is simply the impulse delivered by the system divided by the weight (not mass) of the expended propellant. The impulse is measured directly by the test stand, and the propellant consumption is determined by weighing the thruster before and after a test. The specific impulse is calculated with:

$$I_{sp} = \frac{J}{g\Delta m} \qquad\qquad (14)$$

where J is the total impulse applied over the entire test, g is the standard acceleration due to gravity (9.806 m/s^2), and Δm is the propellant mass consumed by the thruster. This has an associated uncertainty of:

$$\sigma_{Isp}^2 = \sigma_J^2 \left(\frac{1}{g\Delta m}\right)^2 + \sigma_{\Delta m}^2 \left(\frac{J}{g\Delta m^2}\right)^2 \qquad (\ 15\ )$$

From this, it can be seen that for a given uncertainty in applied impulse and mass loss (for example, scale precision), increasing the total firing time will increase J and Δm proportionally, and reduce the total uncertainty. However, because the uncertainties in sequential pulses are not independent, σ_J increases with J as more pulses are added, and the first term is nearly unaffected. As total firing time increases, the second term will become negligible, and the uncertainty in the I_{sp} will be dominated by the uncertainty in J. Because of this, specific impulse tests require numerous pulses to achieve a J and Δm large enough to sufficiently to reduce the magnitude of the second term below that of the first. A typical I$_{sp}$ test for the BioSentinel thruster involved between 5,000 and 10,000 pulses, each one between 10 and 50 milliseconds. The thruster was determined to have an I_{sp} of 44.1 ± 2.1 s.

VI. Conclusion

A low-cost thrust test stand was designed and constructed at Georgia Tech's Space Systems Design Lab to support research into propulsion systems for small satellites. The stand uses a torsional pendulum design to accurately measure small impulses. This stand has been used to determine average thrust level and specific impulse of an attitude control thruster for NASA's BioSentinel mission. The ability to perform in-house testing of thrust and specific impulse on SSDL-made thrusters has greatly simplified the development of these thrusters, without the expense of using a professional system.

References

[1] Kolbeck, J., et al, "uCAT Micro-Propulsion Solution for Autonomous Mobile On-Orbit Diagnostic System," 30th Annual AIAA/USU Conference on Small Satellites, Logan, UT, 2016.

[2] Palmer, K., Sundqvist, J., Zaldivar, A. S., and Gronland, T., "In-Orbit Demonstration of a MEMS-based Micropropulsion System for Cubesats," 30th Annual AIAA/USU Conference on Small Satellites, Logan, UT, 2016.

[3] Polk, J., Pancotti, A., Haag, T., King, S., Walker, M., Blakely, J., and Ziemer, J., "Recommended Practices in Thrust Measurements," 33rd International Electric Propulsion Conference, Fairview Park, OH: Electric Rocket Propulsion Society, IEPC Paper 2013-440, 2013.

[4] Haag, T. W., "PPT Thrust Stand," 31st AIAA/ASME/SAE/ASEE Joint Propulsion Conference and Exhibit, San Diego, CA, 1995.

[5] Sorgenfrei, M., Stevenson, T., and Lightsey, G., "Performance Characterization of a Cold Gas Propulsion System for a Deep Space Cubesat," 40th Annual AAS Guidance and Control Conference, Breckenridge, CO, 2017.

American Institute of Aeronautics and Astronautics